The evolution of pelvic canal shape and rotational birth in humans

Ekaterina Stansfield (katya.stansfield@univie.ac.at)
University of Vienna https://orcid.org/0000-0001-8548-0995
Barbara Fischer
University of Vienna https://orcid.org/0000-0002-4492-8906
Philipp Mitteroecker
University of Vienna

Biological Sciences - Article

Keywords: Mediolaterally Oval Shape, Anteroposteriorly Oval Shape, Pelvic Floor Stability

Posted Date: May 11th, 2021

DOI: https://doi.org/10.21203/rs.3.rs-495939/v1

Abstract

The human foetus needs to rotate when passing through the tight birth canal because of the complex shape of the pelvis. In most women the upper part, or inlet, of the birth canal has a round or mediolaterally oval shape, which is considered ideal for parturition, but it is unknown why the lower part, or outlet, of the birth canal has a pronounced anteroposteriorly oval shape. Here we show that the shape of the lower birth canal affects the ability of the pelvic floor to resist pressure exerted by the abdominal organs and the foetus. Based on a series of finite element analyses, we found that the highest deformation, stress and strain occur in pelvic floors with a circular or mediolaterally oval shape, whereas an anteroposterior elongation increases pelvic floor stability. This suggests that the anteroposterior oval outlet shape is an evolutionary adaptation for pelvic floor support. For the pelvic inlet, by contrast, it has long been assumed that the mediolateral dimension is constrained by the efficiency of upright locomotion. But we argue that upright stance limits the anteroposterior dimension of the inlet. A deeper inlet requires greater pelvic tilt and lumbar lordosis, which compromises spine health and the stability of upright posture. These different requirements on the pelvic inlet and outlet have led to the complex shape of the human pelvic canal and to the evolution of rotational birth.

Introduction

The tight fit between the human birth canal and the foetus results in relatively high rates of birth-related morbidities and, in the absence of medical interventions, maternal and foetal mortality [1,2]. Moreover, human childbirth is characterized by a complex rotational motion of the neonate as it passes through the birth canal (Fig 1a). Rotational birth is necessary as the human birth canal is not a uniform structure: its largest dimensions are oriented in different directions in the three planes of the pelvis, the inlet, the midplane, and the outlet (Fig. 1). In most women, the pelvic inlet has its longest diameter in the mediolateral (ML) direction and the midplane is approximately round, but the longest diameter in the outlet is in anteroposterior (AP) direction. This shape difference between the upper and lower birth canal mainly owes to the medially protruding ischial spines in the midplane and the ischial tuberosities as well as the outward projecting sacrum in the outlet. In physiological vaginal birth, the foetus presents by the head and aligns the largest dimension of its head (the sagittal direction) with the longest diameters of the maternal birth canal in the three planes by rotating through the birth canal (Fig. 1) [3–5]. This raises the question as to why midplane and outlet differ in shape from the inlet, thus enforcing the complicated and risky rotational birth process. Presumably, childbirth would be easier if all pelvic planes had the same shape.

Evolutionarily, human pelvic morphology has been the target of many, partly antagonistic selection pressures. The size of the birth canal presumably evolved by trading off the advantage of a large birth canal for childbirth against the disadvantage for bipedal locomotion, thermoregulation, and particularly for pelvic floor support [4,6–15]. Up to 45% of women experience some degree of incontinence or pelvic organ prolapse in their life, especially postpartum, but pelvic floor disorders can also affect young and

nulliparous women [16–19]. Clinical and biomechanical studies [20–24] confirmed that a larger birth canal increases the risk of pelvic floor disorders.

We propose that not only the size but also the shape of the birth canal is subject to functional and evolutionary trade-offs between parturition, pelvic floor stability and locomotion. These selective factors, however, differentially affect different parts of the pelvis. The size and shape of the pelvic inlet is particularly decisive for successful parturition. Locomotion efficiency is assumed to be affected by the distance between the acetabula [12,25], which are located close to the inlet and might thus impose an indirect selection pressure on inlet form. Selection for pelvic floor function acts on the lower birth canal (midplane and outlet), which provides the attachment points for the pelvic floor tissues [6,26]. A circular or slightly mediolaterally oval inlet ("gynecoid" pelvis) seems to be advantageous for parturition and is most frequent in females [27–29]. For instance, Betti and Manica [30] reported that the mean AP/ML ratio of the pelvic inlet ranges from 0.78 to 0.94 across 20 human populations, whereas the ratio of AP diameter in the outlet to ML diameter in the midplane (which best represents the dimensions of the pelvic floor) ranges from 1.10 to 1.28. Why is the longest dimension of the outlet not aligned with the longest dimension of the inlet, thus requiring the foetus to perform a complex rotation to pass the birth canal? What is the advantage of a 'twisted' birth canal?

Stansfield et al. [24] demonstrated that the deformation of the pelvic floor in response to pressure increases with the average radius of the pelvic floor, making women with a larger birth canal more susceptible to pelvic floor dysfunction. When idealizing the pelvic floor as an elliptically shaped elastic membrane that varies in eccentricity, a circular pelvic floor has a larger minimal diameter than an oval pelvic floor of the same area. In other words, an elliptical shape of the pelvic floor keeps some of the fibres (those along the minor axis of the ellipse) shorter compared to a circular shape of the same area. This, in turn, may reduce pelvic floor deformation under pressure. Hence, we propose that even though a round inlet is advantageous for childbirth, an oval outlet is advantageous for pelvic floor support.

We tested this hypothesis by a series of finite element analyses (FEA) of idealized pelvic floor models that vary from oval to round, while keeping the area and thickness constant. Loaded with an increased physiological intra-abdominal pressure (typical of Valsalva manoeuvre), we observed the magnitude of deformation (maximal displacement), stress and strain in the pelvic floor for the differently shaped pelvic floor models. To disentangle the biomechanical effects of pelvic floor geometry from those of the material properties, we study three different geometric idealizations of the pelvic floor: a flat membrane, a regular 3D oval-shaped hammock, and an anatomically more realistic shape (referred to as 'flat', 'ellipsoid', 'anatomical' models; Fig. 2).

Results

For the flat and ellipsoid models, the highest values of displacement, stress and strain were found in models with a circular shape (Fig. 3). Overall, the flat models displaced about three times as much as the

ellipsoid models and experienced higher stresses and strains (Fig. 3). Introduction of gravity to the finite element analyses increased displacement, stress and strain by a small amount only.

In the anatomical model, most of the deformation occurred in two separate centres, which correspond to the anterior (between the pubis and the boundary between the anterior and posterior walls of vagina) and posterior (the posterior wall of vagina, rectum and post-rectum area) pelvic floor compartments (Fig. 2a). Total displacement was higher in the anterior compartment than in the posterior compartment (Fig. 3), whereas strains and stresses were higher in the posterior compartment. In contrast to the flat and ellipsoid models, the highest displacement of the anatomical model occurred at an AP/ML ratio of 0.83, while models with AP/ML=0.71 experienced the highest stresses and strains (Fig. 3). The introduction of gravity slightly increased displacement, stress, and strain.

For all three geometries, the material properties followed the same trajectory of the stress-strain relationship (SI Fig. 1a). The material stiffness was linear for the experimental pressure of 4kPa and slightly nonlinear for a pressure of 20kPa. Nonetheless, also for the higher pressure all three model types showed the same stress-strain relationship (SI Fig. 1b). This indicates that the biomechanical differences between anatomical, flat and ellipsoid geometries are due to their differences in shape, rather than due to the non-linear effect of the numerical model of the material (see Methods).

Discussion

In agreement with our hypothesis, we found that the ability to resist pressure is indeed affected by the shape of the female pelvic floor, as delimited by the lower birth canal. For flat and ellipsoid models, a circular shape led to the highest displacements. Deviation from circularity in either the anteroposterior (AP) or mediolateral (ML) direction equally reduced deformation, stress and strain. This symmetrical behaviour results from the geometrical symmetry of the flat and ellipsoid models as well as from the isotropic material properties adopted here (see Methods). The curvature of the ellipsoid model also resulted in considerably less displacement, stress and strain. For the more realistic anatomical model, by contrast, the AP cross-section was not symmetrically shaped, with the maximum curvature located at the area of the anal sphincter. As a result, the highest deformation was not observed for a circular model but for a mediolaterally elongated shape with AP/ML=0.83. The highest values of strain and stress occurred in models with AP/ML=0.71. An even more extreme ML oval shape only weakly reduced displacement, stress, and strain. However, increasing the AP/ML ratio towards a more AP oval shape of the anatomical model led to a rapid decrease in all three measures. As our anatomical model still is an idealization of the real pelvic floor, the actual pelvic floor shape leading to the greatest deformation may deviate from our estimate but is likely to have an AP/ML ratio smaller than 1 (see Validation in the Methods).

These findings suggest that a mediolaterally elongated shape of the pelvic midplane and outlet is particularly disadvantageous for pelvic floor support. The more anteroposteriorly oval the lower birth canal is, the more resistant is the pelvic floor in response to pressure. This is in agreement with clinical literature reporting that a mediolaterally wide pelvic outlet predisposes to pelvic floor dysfunction [20,31–33].

Based on these findings, we suggest that the length and orientation of the ischial spines and the sacrum specifically evolved to decouple the shape of the lower birth canal from that of the upper canal in order to ensure a pelvic floor shape that increases the mechanical stability of the pelvic floor.

The stability of the pelvic floor does not only depend on its size and shape. Parity, mode of delivery, age, obesity, and weakness or injuries of pelvic floor tissue are important risk factors for pelvic floor disorders [22,34–36]. However, all these factors presumably are uncorrelated with pelvic canal shape and thus are able to evolve independently. In other words, the presence of other, clinically more relevant factors does not rule out that the shape of the lower birth canal has an effect on pelvic floor stability. In turn, this implies that pelvic floor stability imposes a selective pressure on the shape of the pelvic canal. Although pelvic form is influenced by nutrition during childhood and adolescence, age of menarche, and maternal age at birth, it has a relatively high heritability [37] and thus is expected to respond to the selection imposed by pelvic floor stability.

Our findings explain why the lower birth canal evolved an AP oval shape. But why did the inlet not evolve a similar AP oval shape? After all, a uniformly shaped birth canal would ease parturition as it would make rotational birth obsolete. In humans, a balanced upright stance requires a curved spine, particularly a pronounced lumbar lordosis, which brings the centre of mass of the upper body above the line connecting the two hip joints. In this way, the body is pivoted at the hip joints and balanced antero-posteriorly. An increase in AP length of the pelvis requires re-balancing this system by forward rotating the sacrum and increasing lumbar lordosis (Fig. 4) [38–41]. The amount of lordosis, however, is limited by the size, strength and wedging of the vertebral bodies as well as by necessary adaptations within the spinal musculature. A large lordotic angle increases anterior shearing strain in the vertebrae and intervertebral disks, and it brings the centre of mass anterior to the sacral endplate, both of which are associated with back pain, spondylolisthesis and disk herniation [42–46]. In late pregnancy, lumbar lordosis is further increased to balance the additional abdominal weight [47]. We therefore suggest that an evolutionary increase in AP length of the pelvic inlet has been constrained by the adverse effects it would have on spine health and structural stability of upright posture. Since Washburn's seminal article on the "obstetrical dilemma" [48], researchers have been asking why humans did not evolve a ML wider pelvic inlet to ease birth. Washburn and many later researchers assumed that the energetics of efficient upright walking constrain the evolution of a ML wider pelvis (but see [49]). However, the fact that most women do have a ML oval inlet implies that the constraint on the ML dimension of the inlet is less severe than that on the AP dimension. Indeed, recent studies found little or no energetic disadvantage associated with a mediolaterally wide pelvis [13,47,50]. Given this tight biomechanical constraint on the AP diameter of the inlet, a further ML elongation may simply contribute little to ease childbirth. As expected under this hypothesis, the particularly AP narrow pelvis of the bipedal australopithecines was associated with a lower lordotic angle (41° versus an average of 51° in humans [51]). Chimpanzees, on the contrary, can biomechanically 'afford' a pronounced AP oval inlet because they are mostly quadrupedal and do not need to balance their weight above the hip joints.

These spinopelvic relationships also shed light on the human sex differences in lumbar lordosis and vertebral wedging, which tend to be greater in females than in males [47,52,53]. Whitcome et al. [47] proposed that this dimorphism, which was already present in early *Homo* and partly even in *Australopithecus*, evolved as an adaptation to mitigate the shearing forces generated by foetal load. However, we suggest that the increased female lordosis and vertebral wedging are, at least partly, a direct consequence of the larger pelvic canal (including the inlet AP diameter) in females [8,54]. Only if the average female lordosis exceeds the degree of lordosis expected for female pelvic dimensions, would an adaption for foetal load be a plausible explanation. But this remains to be shown.

The size of the pelvic canal is certainly more important for parturition and pelvic floor support than its shape. For instance, the increase in pelvic floor displacement resulting from 1 SD (standard deviation) increase in pelvic floor *size* (reported by Stansfield et al. [24]) is about 2.8 times as large as the displacement resulting from 1 SD increase in pelvic floor *shape* (AP/ML). Nonetheless, our results suggest that the shape of the lower birth canal is subject to an evolutionary trade-off between childbirth, pelvic floor support and upright posture, similar to that for the size of the canal: An even more anteroposteriorly oval-shaped lower birth canal would be advantageous for pelvic floor stability but disadvantageous for childbirth; an AP oval inlet would ease parturition by avoiding rotation of the foetus but would compromise structural stability of upright posture and locomotion. However, the relative strengths and actual trade-off dynamics of these antagonistic selective forces depend on biological, environmental and sociocultural factors that have changed during human history and partly differ among populations today ("shifting trade-off model") [55]. For instance, pelvic size as well as neonatal weight and head circumference differ considerably across populations, leading to variable magnitudes of obstetric selection on pelvic form [56–58]. Prevalence of pelvic organ prolapse and incontinence vary across countries as well as by ethnicity and sociocultural background [59–61], imposing different strengths of selection for pelvic floor support. Physical activities and diet differ among populations and cultures, thus exerting different physical stresses on the pelvis and the pelvic floor [e.g., 59] and providing different metabolic capacities during pregnancy [49]. Transitions in environmental and socioeconomic conditions can also affect the relationship between foetal and maternal size, which influences the difficulty of labour [62,63]. Hence, it is likely that the observed population differences in pelvic shape [30] partly resulted from local differences in selective pressures.

References

1. Dolea, C. & AbouZahr, C. Global burden of obstructed labour in the year 2000. *World Health Organization* 1–17 (2003).
2. Neilson, J. P., Lavender, T., Quenby, S. & Wray, S. Obstructed labour. *Br. Med. Bull.* **67**, 191–204 (2003).
3. Rosenberg, K. & Trevathan, W. Birth, obstetrics and human evolution. *BJOG* **109**, 1199–1206 (2002).

4. Wittman, A. B. & Wall, L. L. The evolutionary origins of obstructed labor: bipedalism, encephalization, and the human obstetric dilemma. *Obstet. Gynecol. Surv.* **62**, 739–748 (2007).
5. Collins, S., Arulkumaran, S., Hayes, K. & Jackson, S. *Oxford Handbook of Obstetrics and Gynaecology*. (OUP Oxford, 2008).
6. Abitbol, M. Evolution of the Ischial Spine and of the Pelvic Floor in the Hominoidea. *Am. J. Phys. Anthropol.* **75**, 53–67 (1988).
7. Lovejoy, C. O. Evolution of human walking. *Sci. Am.* **259**, 118–125 (1988).
8. Tague, R. G. Sexual dimorphism in the human bony pelvis, with a consideration of the Neandertal pelvis from Kebara Cave, Israel. *Am. J. Phys. Anthropol.* **88**, 1–21 (1992).
9. Ruff, C. Variation in Human Body Size and Shape. *Annu. Rev. Anthropol.* **31**, 211–232 (2002).
10. Rosenberg, K. & Trevathan, W. Bipedalism and human birth: The obstetrical dilemma revisited. *Evolutionary Anthropology* **4**, 161–168 (2005).
11. Mitteroecker, P., Huttegger, S. M., Fischer, B. & Pavlicev, M. Cliff-edge model of obstetric selection in humans. *Proc. Natl. Acad. Sci. U. S. A.* **113**, 14680–14685 (2016).
12. Ruff, C. Mechanical Constraints on the Hominin Pelvis and the 'Obstetrical Dilemma'. *Anat. Rec.* **300**, 946–955 (2017).
13. Gruss, L. T., Gruss, R. & Schmitt, D. Pelvic Breadth and Locomotor Kinematics in Human Evolution. *Anat. Rec.* **300**, 739–751 (2017).
14. Grunstra, N. D. S. *et al.* Humans as inverted bats: A comparative approach to the obstetric conundrum. *Am. J. Hum. Biol.* e23227 (2019).
15. Pavličev, M., Romero, R. & Mitteroecker, P. Evolution of the human pelvis and obstructed labor: new explanations of an old obstetrical dilemma. *Am. J. Obstet. Gynecol.* **222**, 3–16 (2020).
16. Dietz, H. P. & Clarke, B. Prevalence of rectocele in young nulliparous women. *Aust. N. Z. J. Obstet. Gynaecol.* **45**, 391–394 (2005).
17. Kenton, K. & Mueller, E. R. The global burden of female pelvic floor disorders. *BJU Int.* **98**, 1–5 (2006).
18. Nygaard, I. *et al.* Prevalence of symptomatic pelvic floor disorders in US women. *JAMA* **300**, 1311–1316 (2008).
19. Lawrence, J. M., Lukacz, E. S., Nager, C. W., Hsu, J.-W. Y. & Luber, K. M. Prevalence and co-occurrence of pelvic floor disorders in community-dwelling women. *Obstet. Gynecol.* **111**, 678–685 (2008).
20. Sze, E. H., Kohli, N., Miklos, J. R., Roat, T. & Karram, M. M. Computed tomography comparison of bony pelvis dimensions between women with and without genital prolapse. *Obstet. Gynecol.* **93**, 229–232 (1999).
21. Handa, V. L. *et al.* Architectural differences in the bony pelvis of women with and without pelvic floor disorders. *Obstetrics & Gynecology* **102**, 1283–1290 (2003).
22. Brown, K. M., Handa, V. L., Macura, K. J. & DeLeon, V. B. Three-dimensional shape differences in the bony pelvis of women with pelvic floor disorders. *Int. Urogynecol. J.* **24**, 431–439 (2013).

23. Sammarco, A. G. *et al.* Pelvic cross-sectional area at the level of the levator ani and prolapse. *Int. Urogynecol. J.* **32**, 1007–1013 (2021).
24. Stansfield, E., Kumar, K., Mitteroecker, Philipp & Grunstra, N. D. S. Biomechanical trade-offs in the pelvic floor constrain the evolution of the human birth canal. *PNAS* (2021).
25. Lovejoy, C. O. The natural history of human gait and posture. *Gait Posture* **21**, 95–112 (2005).
26. Herschorn, S. Female Pelvic Floor Anatomy: The Pelvic Floor, Supporting Structures, and Pelvic Organs. *Rev. Urol.* **6(suppl 5)**, 2–10 (2004).
27. Caldwell, W. E. & Moloy, H. C. Anatomical variation in the female pelvis: their classification and obstetrical significance. *Proceedings of the Royal Society of Medicine. Section of Obstetrics and Gynaecology.* **32**, 1–30 (1938).
28. Maharaj, D. Assessing cephalopelvic disproportion: back to the basics. *Obstet. Gynecol. Surv.* **65**, 387–395 (2010).
29. Stewart, K. S., Cowan, D. B. & Philpott, R. H. Pelvic dimensions and the outcome of trial labour in Shona and Zulu primigravidas. *S. Afr. Med. J.* **55**, 847–851 (1979).
30. Betti, L. & Manica, A. Human variation in the shape of the birth canal is significant and geographically structured. *Proc. Biol. Sci.* **285**, (2018).
31. Stav, K. *et al.* Pelvis architecture and urinary incontinence in women. *Eur. Urol.* **52**, 239–244 (2007).
32. Xu, H.-N. *et al.* Investigation of correlation between diameters of pelvic inlet and outlet planes and female pelvic floor dysfunction. *Eur. J. Obstet. Gynecol. Reprod. Biol.* **159**, 461–464 (2011).
33. Berger, M. B., Doumouchtsis, S. K. & DeLancey, J. O. Bony pelvis dimensions in women with and without stress urinary incontinence. *Neurourol. Urodyn.* **32**, 37–42 (2013).
34. Blomquist, J. L., Muñoz, A., Carroll, M. & Handa, V. L. Association of Delivery Mode With Pelvic Floor Disorders After Childbirth. *JAMA* **320**, 2438–2447 (2018).
35. Lukacz, E. S., Lawrence, J. M., Contreras, R., Nager, C. W. & Luber, K. M. Parity, mode of delivery, and pelvic floor disorders. *Obstet. Gynecol.* **107**, 1253–1260 (2006).
36. Wu, J. M. *et al.* Prevalence and trends of symptomatic pelvic floor disorders in U.S. women. *Obstet. Gynecol.* **123**, 141–148 (2014).
37. Sharma, K. Genetic basis of human female pelvic morphology: a twin study. *Am. J. Phys. Anthropol.* **117**, 327–333 (2002).
38. Roussouly, P. & Pinheiro-Franco, J. L. Biomechanical analysis of the spino-pelvic organization and adaptation in pathology. *Eur. Spine J.* **20 Suppl 5**, 609–618 (2011).
39. Boulay, C. *et al.* Pelvic incidence: a predictive factor for three-dimensional acetabular orientation-a preliminary study. *Anat. Res. Int.* **2014**, 594650 (2014).
40. Laouissat, F., Sebaaly, A., Gehrchen, M. & Roussouly, P. Classification of normal sagittal spine alignment: refounding the Roussouly classification. *Eur. Spine J.* **27**, 2002–2011 (2018).
41. Pizones, J. & García-Rey, E. Pelvic motion the key to understanding spine-hip interaction. *EFORT Open Rev* **5**, 522–533 (2020).

42. von Lackum, H. L. THE LUMBOSACRAL REGION: AN ANATOMIC STUDY AND SOME CLINICAL OBSERVATIONS. *JAMA* **82**, 1109–1114 (1924).
43. Labelle, H., Mac-Thiong, J.-M. & Roussouly, P. Spino-pelvic sagittal balance of spondylolisthesis: a review and classification. *Eur. Spine J.* **20 Suppl 5**, 641–646 (2011).
44. Caglayan, M. *et al.* Effects of Lumbosacral Angles on Development of Low Back Pain. *J. Musculoskelet. Pain* **22**, 251–255 (2014).
45. Sorensen, C. J., Norton, B. J., Callaghan, J. P., Hwang, C.-T. & Van Dillen, L. R. Is lumbar lordosis related to low back pain development during prolonged standing? *Man. Ther.* **20**, 553–557 (2015).
46. Yu, C. *et al.* Risk Factors for Recurrent L5-S1 Disc Herniation After Percutaneous Endoscopic Transforaminal Discectomy: A Retrospective Study. *Med. Sci. Monit.* **26**, e919888 (2020).
47. Whitcome, K. K., Shapiro, L. J. & Lieberman, D. E. Fetal load and the evolution of lumbar lordosis in bipedal hominins. *Nature* **450**, 1075–1078 (2007).
48. Washburn, S. L. Tools and human evolution. *Sci. Am.* **203**, 63–75 (1960).
49. Dunsworth, H. M., Warrener, A. G., Deacon, T., Ellison, P. T. & Pontzer, H. Metabolic hypothesis for human altriciality. *Proc. Natl. Acad. Sci. U. S. A.* **109**, 15212–15216 (2012).
50. Warrener, A. G., Lewton, K. L., Pontzer, H. & Lieberman, D. E. A wider pelvis does not increase locomotor cost in humans, with implications for the evolution of childbirth. *PLoS One* **10**, e0118903 (2015).
51. Been, E., Gómez-Olivencia, A. & Kramer, P. A. Lumbar lordosis of extinct hominins. *Am. J. Phys. Anthropol.* **147**, 64–77 (2012).
52. Bailey, J. F., Sparrey, C. J., Been, E. & Kramer, P. A. Morphological and postural sexual dimorphism of the lumbar spine facilitates greater lordosis in females. *J. Anat.* **229**, 82–91 (2016).
53. García-Martínez, D. *et al.* Sexual dimorphism in the vertebral wedging of the human lumbar vertebrae and its importance as a comparative framework for understanding the wedging pattern of Neanderthals. *Quat. Int.* **566-567**, 224–232 (2020).
54. Kurki, H. K. Pelvic dimorphism in relation to body size and body size dimorphism in humans. *J. Hum. Evol.* **61**, 631–643 (2011).
55. Mitteroecker, P., Grunstra, N. D. S., Stansfield, E., Waltenberger, L. & Fischer, B. Did population differences in human pelvic form evolve by drift or selection? *Bulletins et mémoires de la Société d'anthropologie de Paris* **33**, 11–26 (2021).
56. Meredith, H. V. Body weight at birth of viable human infants: a worldwide comparative treatise. *Hum. Biol.* **42**, 217–264 (1970).
57. Mikolajczyk, R. T. *et al.* A global reference for fetal-weight and birthweight percentiles. *Lancet* **377**, 1855–1861 (2011).
58. Villar, J. *et al.* International standards for newborn weight, length, and head circumference by gestational age and sex: the Newborn Cross-Sectional Study of the INTERGROWTH-21st Project. *Lancet* **384**, 857–868 (2014).

59. Walker, G. J. A. & Gunasekera, P. Pelvic organ prolapse and incontinence in developing countries: review of prevalence and risk factors. *Int. Urogynecol. J.* **22**, 127–135 (2011).
60. Vergeldt, T. F. M., Weemhoff, M., IntHout, J. & Kluivers, K. B. Risk factors for pelvic organ prolapse and its recurrence: a systematic review. *Int. Urogynecol. J.* **26**, 1559–1573 (2015).
61. Islam, R. M., Oldroyd, J., Rana, J., Romero, L. & Karim, M. N. Prevalence of symptomatic pelvic floor disorders in community-dwelling women in low and middle-income countries: a systematic review and meta-analysis. *Int. Urogynecol. J.* **30**, 2001–2011 (2019).
62. Wells, J. C. K., DeSilva, J. M. & Stock, J. T. The obstetric dilemma: an ancient game of Russian roulette, or a variable dilemma sensitive to ecology? *Am. J. Phys. Anthropol.* **149 Suppl 55**, 40–71 (2012).
63. Zaffarini, E. & Mitteroecker, P. Secular changes in body height predict global rates of caesarean section. *Proc. Biol. Sci.* **286**, 20182425 (2019).

Methods

We assessed how changes in the ratio of anteroposterior to mediolateral diameters of the pelvic floor affect the amount of displacement under physiological pressure conditions. We used three different idealizations of the pelvic floor geometry: a flat membrane, a regular 3D oval-shaped hammock, and a 3D membrane that resembles the real pelvic floor geometry as it is suspended in the midplane and outlet of the birth canal. We refer to the first model as ‘flat’, the second model as ‘ellipsoid’, and the third model as ‘anatomical’ (Fig.2). The shape of the transverse outline of each of the three models was then varied from the mediolaterally wide to the anteroposteriorly long and loaded with pressure from above.

3D geometry

Computer-aided design (CAD) models of the pelvic floor were created as shells in SOLIDWORKS (© 1995-2019 Dassault Systémes). Their mediolateral (ML) diameter corresponded to the distance between the ischial bones at the points of muscle insertion on the ischial spines and was thus equal to the width of the midplane of the birth canal (Fig.1c). The anteroposterior (AP) diameter of each model corresponded to the distance from the inferior point at the pubic symphysis to the apex of the fifth sacral vertebra, which was equal to the length of the outlet of the birth canal in the sagittal view (Fig. 1b).

The transverse diameters of our models were based on the means and standard deviations (SD) of modern Europeans as reported by DelPrete (2019). The base model was assigned the average values of the ML and AP diameters. To create further models, we varied ML diameter in steps of 0.5 or 1.0 standard deviations (SD), while surface area was kept constant by a corresponding change of the AP diameter. In total, 23 models whose ML diameter ranged from -4.5 to +8 SD from the mean, were created for each of the three experiments (i.e., flat, ellipsoid, or anatomical; SI Tab. 1). This range extends well beyond the variation observable in modern humans, allowing us to assess how extreme pelvic shapes, which may have been selected against in the past, would perform. The ellipsoid and anatomical models were assigned a constant depth of 2.9 mm. The depth was determined as an average value of the

perpendicular distance between the pubo-coccygeal axis and the position of the anal sphincter in sagittal CT scans of 10 female individuals from New Mexico Decedent Image Database collection [1]. The depth of the ellipsoid model was taken perpendicular to the anteroposterior and mediolateral axes at the centroid point. The 3D geometry of the anatomical base model was built following the protocol of Stansfield et al. [2]. Figure 1 demonstrates the fit of the three models in the female birth canal. Details of all models are given in SI Table 1.

Finite element model

FE model

We assigned a uniform thickness of 6 mm and a density of 1.0597 g/cm^3 to each of the models [2,3]. The geometry was discretized using more than 3,000 HEX 8 elements with an average element size of 2 mm. An implicit solution scheme using ANSYS Mechanical (© 2008-2021 ANSYS, Inc.) was adopted to solve the quasi-static loading problem. The boundary conditions were identical across models and involved setting the mobility of the rim to zero in all three directions, while allowing for rotation. A constant pressure of 4kPa was applied from above as an equivalent normal force to the entire superior surface of the mesh. The pressure of 4kPa is an average intra-abdominal pressure produced by a Valsalva (straining) manoeuvre, a technique used in medical diagnostics, where patients make a forceful exhale motion while keeping airways closed. This increases the intra-abdominal pressure in a controlled way without contraction of the pelvic floor muscles [4]. Across all experiments, material properties were kept constant to understand how displacement, stresses, and strains of the pelvic floor changed as a consequence of pelvic floor geometry.

Material properties and model validation

We adopted an isotropic Mooney-Rivlin constitutive law to represent pelvic floor tissues with the following parameters: c_1=26 kPa, c_2=14 kPa [5], and the bulk modulus,
K = 1000 kPa [6]. These material properties have been sourced from published literature [5] and previously used for validation of our 'anatomical' model with the base ML and AP diameters [2].

Experiments and measurements

Separately for the flat, ellipsoid and anatomical geometries and the different AP/ML ratios (SI Table 1), we quantified the mechanical response to the applied pressure of 4kPa. We kept the surface area constant in all experiments. In the ellipsoid and anatomical models, we also kept the depth constant. In addition, we assessed the effect of non-linear material properties by comparing the relationship between stresses and strains in the flat, ellipsoid and 'anatomical' base models when applying experimental pressures of 4kPa and 20kPa.

We measured three variables at the location of maximum displacement to assess the performance of the pelvic floor model: the maximum of the total displacement magnitude (in mm), the maximum Von Mises

strain and the maximum Von Mises stress (in MPa). The engineering term ‘strain’ describes the amount of extension the material experiences per unit length, while ‘stress’ denotes the amount of force experienced by the material per unit of its surface. A large strain magnitude implies that the material was stretched, compressed or sheared to a high degree. At the same time, a large stress signifies a high amount of energy that the material absorbed in order to achieve its deformation. Von Mises stress and strain represent stress and strain components that are used to determine the maximum possible distortion of a material [7]. We ignored stresses and strains at the edges of the models because of our boundary conditions. All experiments were performed both with and without the effect of gravity.

Validation

The geometry of the real human pelvic floor is more complex than our anatomical model as it is neither homogeneous in thickness nor in tissue properties. Additionally, pelvic floor tissue properties vary due to individual genetic differences and change with age, hormonal status, and pelvic floor training [8–14]. They also differ between women with and without urinary incontinence [4,5,15,16]. Our model, however, was successfully validated by measuring displacement of the posterior compartment against published dynamic Magnetic Resonance Imaging data [2] and captures the essence of the behaviour of the female pelvic floor during Valsalva manoeuvre by revealing two main areas of displacement. The maximum displacement of the anterior compartment in our model occurs at the anatomical location of the urogenital hiatus, where fibres of the urogenital diaphragm and the anterior part of the levator ani insert into the urethra and anterior vagina. The maximum displacement of the posterior compartment in our model coincides with the location of the ‘bend’ created between the levator plate and the puborectalis muscle (Fig. 2A). In clinical practice, displacements in these two areas are used for diagnosing pelvic floor tissue health and prolapse [17–21], indicating that our model successfully reproduces the anatomical areas critical for pelvic floor health.

Methods References

1. Edgar, H. J. H. *et al.* New Mexico Decedent Image Database. Office of the Medical Investigator, University of New Mexico. (2020) doi:10.25827/5s8c-n515.
2. Stansfield, E., Kumar, K., Mitteroecker, Philipp & Grunstra, N. D. S. Biomechanical trade-offs in the pelvic floor constrain the evolution of the human birth canal. *PNAS* (2021).
3. Mendez, J. Density and composition of mammalian muscle. *Metabolism* **9**, 184–188 (1960).
4. Silva, M. E. T., Brandão, S., Parente, M. P. L., Mascarenhas, T. & Natal Jorge, R. M. Establishing the biomechanical properties of the pelvic soft tissues through an inverse finite element analysis using magnetic resonance imaging. *Proc. Inst. Mech. Eng. H* **230**, 298–309 (2016).
5. Silva, M. E. T., Brandão, S., Parente, M. P. L., Mascarenhas, T. & Natal Jorge, R. M. Biomechanical properties of the pelvic floor muscles of continent and incontinent women using an inverse finite element analysis. *Comput. Methods Biomech. Biomed. Engin.* **20**, 842–852 (2017).

6. Maas, S. A., Ellis, B. J., Ateshian, G. A. & Weiss, J. A. FEBio: finite elements for biomechanics. *J. Biomech. Eng.* **134**, 011005 (2012).
7. Oomens, C., Brekelmans, M. & Baaijens, F. *Biomechanics, Concepts and Computations*. (Cambridge University Press, 2010).
8. Bernstein, I. T. The pelvic floor muscles: muscle thickness in healthy and urinary-incontinent women measured by perineal ultrasonography with reference to the effect of pelvic floor training. Estrogen receptor studies. *Neurourol. Urodyn.* **16**, 237–275 (1997).
9. Tinelli, A. *et al.* Age-related pelvic floor modifications and prolapse risk factors in postmenopausal women. *Menopause* **17**, 204–212 (2010).
10. Dehghan, F. *et al.* The effect of relaxin on the musculoskeletal system. *Scand. J. Med. Sci. Sports* **24**, e220–9 (2014).
11. Bhattarai, A. & Staat, M. Modelling of Soft Connective Tissues to Investigate Female Pelvic Floor Dysfunctions. *Comput. Math. Methods Med.* **2018**, 9518076 (2018).
12. Bodner-Adler, B., Alarab, M., Ruiz-Zapata, A. M. & Latthe, P. Effectiveness of hormones in postmenopausal pelvic floor dysfunction-International Urogynecological Association research and development-committee opinion. *Int. Urogynecol. J.* (2019) doi:10.1007/s00192-019-04070-0.
13. Bø, K. & Nygaard, I. E. Is Physical Activity Good or Bad for the Female Pelvic Floor? A Narrative Review. *Sports Med.* **50**, 471–484 (2020).
14. Liapis, I. *et al.* Expression and importance of relaxin in vaginal wall tissues from women with pelvic organ prolapse and with/without stress urinary incontinence. *Clin. Obstet. Gynecol. Reprod. Med.* **6**, (2020).
15. Ruiz-Zapata, A. M. *et al.* Biomechanical Properties of the Pelvic Floor and its Relation to Pelvic Floor Disorders. *European Urology Supplements* **17**, 80–90 (2018).
16. Egorov, V. *et al.* Biomechanical mapping of the female pelvic floor: changes with age, parity and weight. *Pelviperineology* **38**, 3–11 (2019).
17. El Sayed, R. F. *et al.* Magnetic resonance imaging of pelvic floor dysfunction - joint recommendations of the ESUR and ESGAR Pelvic Floor Working Group. *Eur. Radiol.* **27**, 2067–2085 (2017).
18. Fernández, M. M., Molina, A. & Valtorta., Á. Dynamic MRI of the pelvic floor: Its usefulness at prolapse. *Revista Argentina de Diagnóstico por Imágenes* **4**, 6–12 (2015).
19. Lockhart, M. E., Bates, G. W., Morgan, D. E., Beasley, T. M. & Richter, H. E. Dynamic 3T pelvic floor magnetic resonance imaging in women progressing from the nulligravid to the primiparous state. *Int. Urogynecol. J.* **29**, 735–744 (2018).
20. Arif-Tiwari, H. *et al.* Improved Detection of Pelvic Organ Prolapse: Comparative Utility of Defecography Phase Sequence to Nondefecography Valsalva Maneuvers in Dynamic Pelvic Floor Magnetic Resonance Imaging. *Curr. Probl. Diagn. Radiol.* **48**, 342–347 (2019).
21. Talasz, H. *et al.* Phase-locked parallel movement of diaphragm and pelvic floor during breathing and coughing-a dynamic MRI investigation in healthy females. *Int. Urogynecol. J.* **22**, 61–68 (2011).

Declarations

Acknowledgements

This work was supported by a Lise Meitner grant (M-2772-B) and an Elise Richter grant (V 826-B) from the Austrian Science Fund (FWF) to Ekaterina Stansfield and Barbara Fischer, respectively. We are grateful to Krishna Kumar, Nicole Grunstra and Maria Vila Pouca, who contributed fruitful critique and discussions on the finite element modelling of the pelvic floor. We thank Eva Zaffarini for drawing Figure 1.

Author contributions

K.S. and P.M. designed the research; K.S. performed the analyses; K.S., B.F. and P.M. interpreted the results and wrote the paper.

Competing interests

The authors declare no competing interests.

Figures

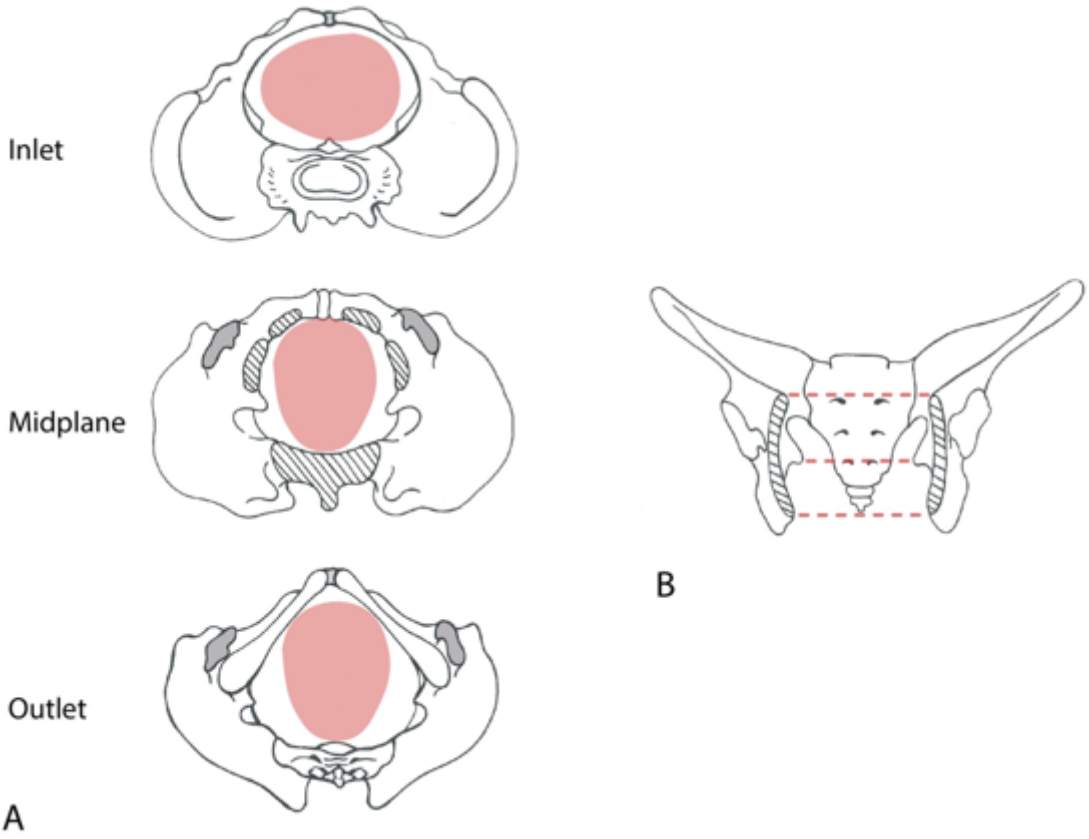

Figure 1

Rotational birth in humans. (A) The foetal head engages in transverse direction and rotates about 90° to align its maximum dimension with the largest dimension of each pelvic plane. (B) Pelvic inlet, midplane and outlet in frontal view.

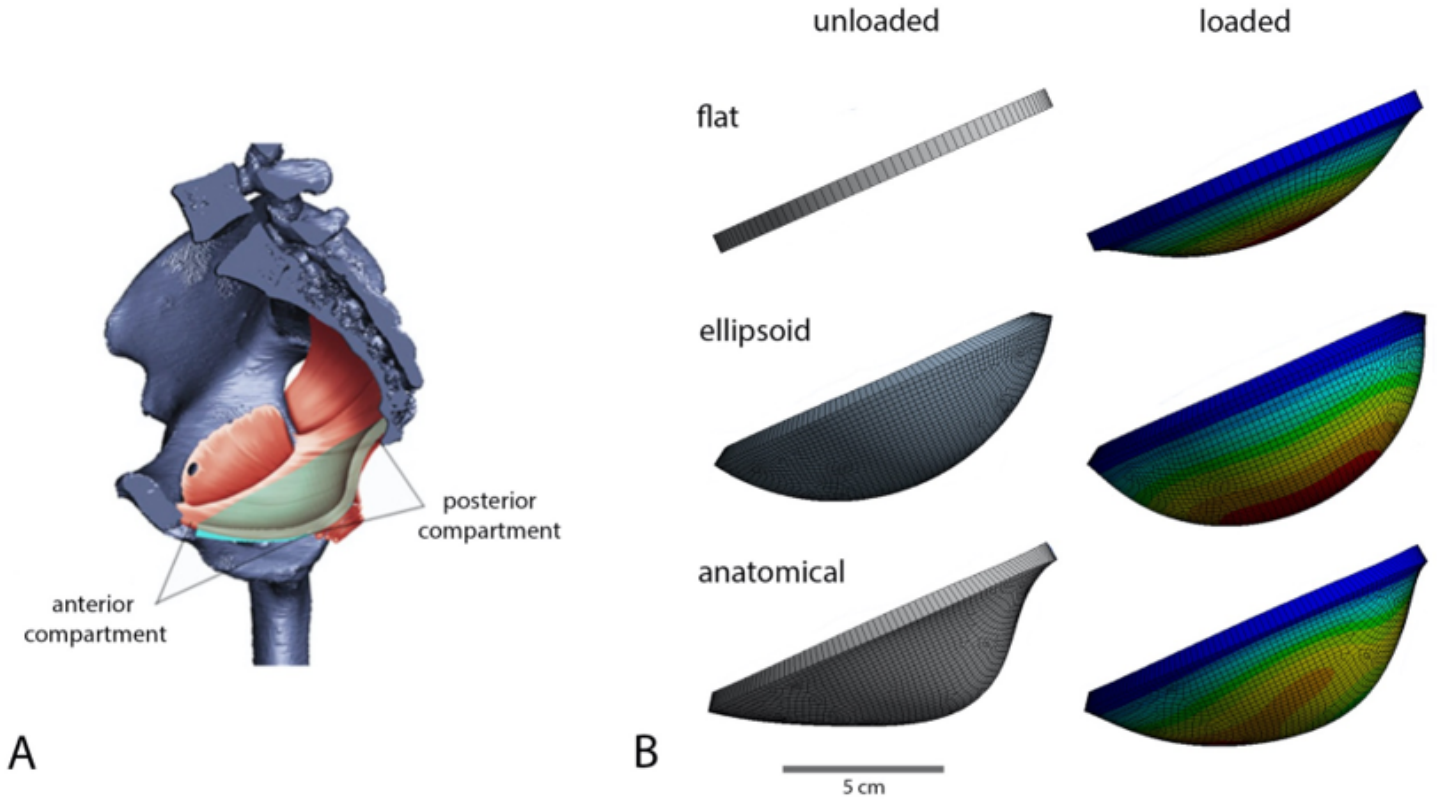

Figure 2

Pelvic floor models for finite element analysis. (A) Anatomical model (cyan colour, superimposed on muscles of the pelvic floor, sagittal view), oriented approximately along the pubococcygeal axis of an upright person. (B) Flat, ellipsoid and anatomical models (sagittal views). In the left column the three models are shown before loading, whereas the right column shows the displacement in response to 4kPa pressure. The rainbow colour scheme indicates the magnitude of the maximum displacement of the model elements. Blue corresponds to no displacement, red to high displacement.

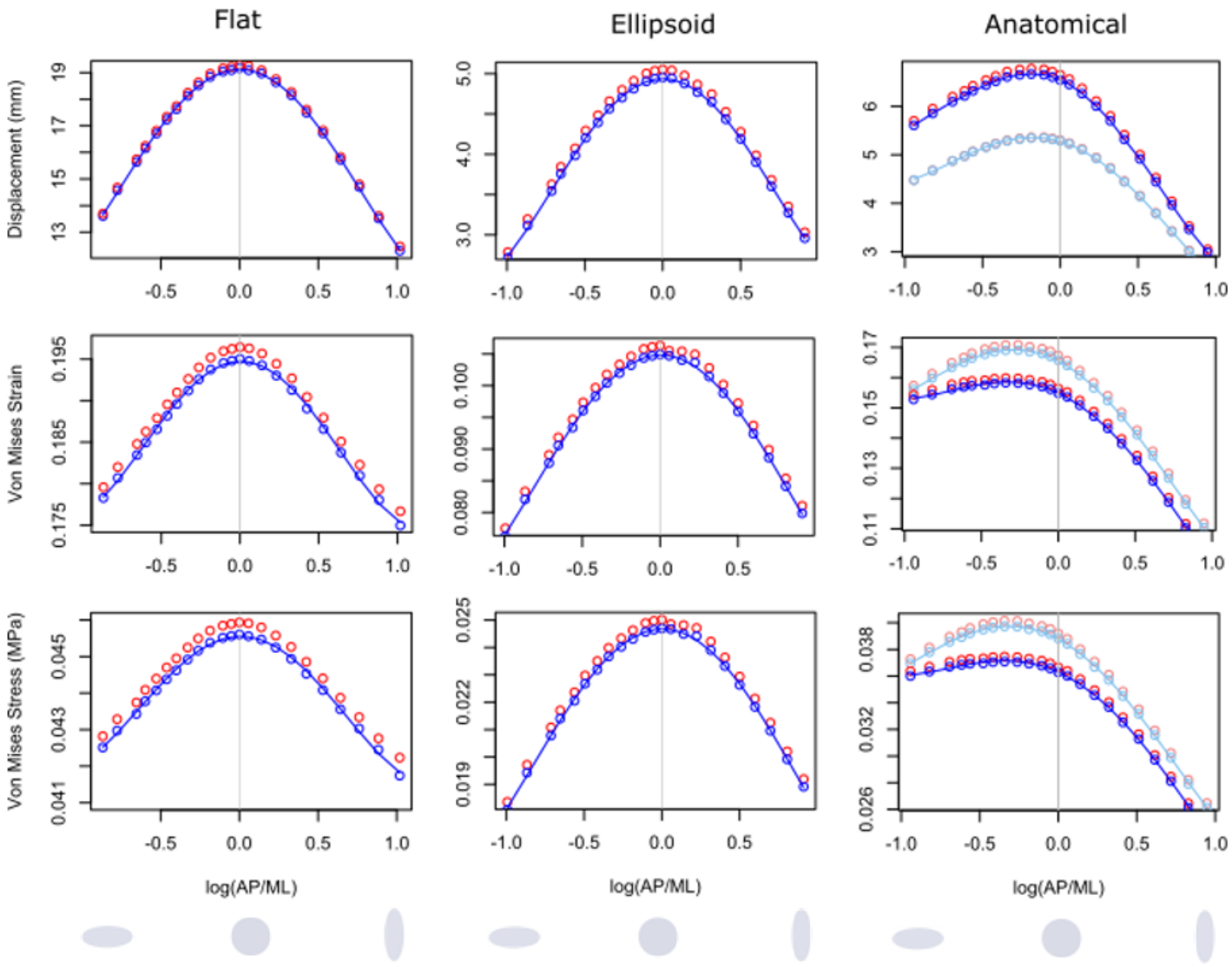

Figure 3

Results of loading experiments (total displacement, maximum Von Mises strain, maximum Von Mises stress) for the three geometries. In each panel, the horizontal axis represents the shape of the pelvic floor models, expressed by the natural logarithm (log) of the ratio AP/ML to guarantee that the same mediolaterally (ML) and anteroposteriorly (AP) oval shapes are equally distant from circularity, i.e., log(AP/ML)=-log(ML/AP). Negative values correspond to ML elongated shapes; positive values to AP elongated shapes (depicted by the grey ellipses). The value log(AP/ML)=0 corresponds to a circular pelvic floor where AP=ML. The blue marks represent the results for an applied pressure of 4 kPa, and the red marks the results for pressure and gravity applied together. In the anatomical model, most of the deformation occurred in two separate centres, corresponding to the anterior and posterior pelvic floor compartments, for which the results are shown separately here (blue/red for the anterior compartment; light blue/light red for the posterior compartment).

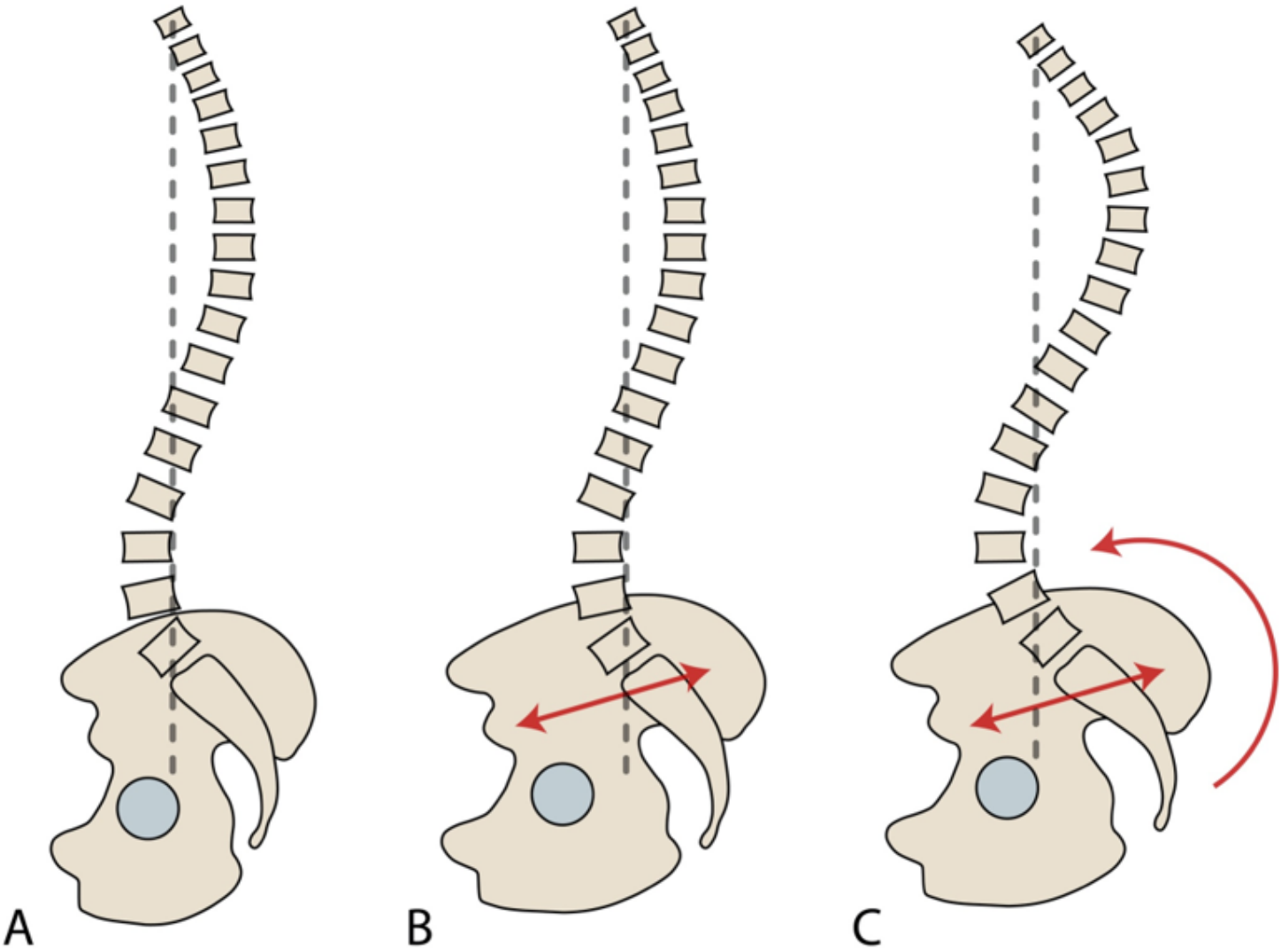

Figure 4

Relationship between pelvic depth and spinal curvature. (A) Schematization of normal spinopelvic relationships, where the centre of mass (as indicated by the dashed line, the C7 plumbline) is positioned sagittally above the hip joints and the superior endplate of the sacrum. (B) In an anteroposteriorly elongated pelvis (as indicated by the red double arrow) without spinal adjustment, the centre of mass is located behind the hip joints, which compromises the structural stability of upright posture. (C) To bring the centre of mass back above the hip joints in this elongated pelvis, the sacrum needs to be anteverted (tilted forward), which leads to an overall increased curvature of the spine, particularly an increased lumbar lordosis, and a deviation of the centre of mass from the sacral endplate. These conditions are associated with multiple orthopaedic disorders.

Supplementary Files

This is a list of supplementary files associated with this preprint. Click to download.

- SupplementaryInformation.docx